Simulation on the Ejection Performance of Thermal Bubble Inkjet Printhead for Top and Back Shooting Design

Jinn-Cherng Yang, Chi-Ming Huang, and Chun-Jung Chen
K200/OES/ITRI, Industrial Technology Research Institute
Chutung, Hsinchu, Taiwan, R. O. C.

Abstract

There are many parameters that influence droplet ejection performance, i.e. printing quality, of inkjet print head such as ejection velocity and directionality of ink droplet. Ink droplet with larger ejection velocity from an inkjet print head nozzle exit will be less affected by the surrounded air disturbance and keep a good directionality. The printing quality of a thermal bubble inkjet print head is also affected by bubble growth dynamics. It depends on the proper geometry and size designs of micro-fluidic ink channel within the inkjet print head such as nozzle orifice, ink firing chamber and heaters. This work used computational fluid dynamics (CFD) method to study the parameters and effects on droplet ejection performance of thermal bubble inkjet print head for both top and back shooting type of thermal bubble nucleation. The numerical scheme, volume of fluid (VOF) method, has been used to deal with the interface between surrounded air and droplet liquid.

Introduction

High dispensing accuracy is an important issue for the highly resolution inkjet printing and industrial printing applications on the manufacture of PLED display, color filter and biochip, etc. There are many parameters that influence droplet ejection performance, i.e. printing quality, of inkjet print head such as ejection velocity and directionality of ink droplet. Ink droplet with larger ejection velocity from an inkjet print head nozzle exit will be less affected by the surrounded air disturbance and keep a good directionality. The printing quality of a thermal bubble inkjet print head is also affected by bubble growth dynamics. Asai et al.[1] conducted both numerical simulation and experimental measurements to obtain the temporal variation of the ejected droplet length. Chen et al.[2] used a one-dimensional model to describe the unsteady conduction problem, bubble growth, and ink motion of the top-shooter thermal inkjet print head. Their results show that the threshold operating voltage for ink ejection decreases with the heat pulse width. Ink droplet with larger ejection velocity from an inkjet print head nozzle exit will be less affected by the surrounded air disturbance and keep a good directionality. Yang et al.[3] present the study with numerical predictions on thermal bubble print head and reveal that a three-step voltage heating condition (with less thermal energy input) results in a larger mean inkjet nozzle exit velocity than the one-step voltage heating method. The larger heat flux rate from the print head heater to the ink chamber results in larger bubble pressure and inkjet exit velocity. It also depends on the proper geometry and size designs of micro-fluidic ink channel within the inkjet print head such as nozzle orifice, ink firing chamber and heaters. Chiu et al.[4] discussed the size effects of the micro fluidic channel on the droplet ejection process. He concluded that the double-feed-channel model is a better design than the single-feed-channel model.

Fabrication methods of the commercial inkjet print head are the dry film layer made of polymeric material is laminated on the chip and forms the ink flow channel pattern by photolithography process. The sandblast process is introduced to form a through slot that passes the chip for ink feeding. Contamination and crack of the silicon wafer are commonly seen during the sandblast process. In addition, the sandblast ink slot on a chip increases the difficulty of the circuit layout. The nozzle plate is then attached to the chip one-on-one by the adhesive characteristic of the dry film. However, the alignment accuracy of the nozzle plate to the chip is limited and hard to control the error within 3 μm. The ejection performance of inkjet print head heavily depends on the accuracy of the bonding process. The back shooting type design of inkjet print head replace the sandblast process by three-dimensional electroforming process, i.e. there is no ink slot needed on the chip. The process will increase the nozzle array density of the inkjet head because there is a larger space for circuit layout in the limited small chip area and one doesn't have to consider how to pass the circuit through the ink slot. This type of back-shooting design could have the high printing quality and it provides a non-assembly packaging process of inkjet head products. It could solve the miss alignment problem between the inkjet chip and nozzle

plate, especially for higher density array of thermal bubble heaters.

The aim of this study is to investigate the factors that affecting the droplet ejection process for both top and back shooting type design. Computational Fluid Dynamics (CFD) method has been applied to study these parameters of thermal bubble nucleation. The numerical scheme, volume of fluid (VOF) method, has been used to deal with the interface between surrounded air and the liquid droplet.

Theoretical Model and Numerical Scheme

The physical properties such as surface tension and viscosity of the working fluid are important factors that affect the droplet ejection behavior. It is necessary to simulate on the ejection performance of the micro-fuel injector with working fluid of gasoline. Theoretically, the ejection of droplet phenomenon is governed by Navier-Stokes equations with appropriate boundary conditions describing fluid interface motions. Volume of fluid (VOF) method resolves the transient motion of the gas and liquid phase using the Navier-Stokes equations, and accounts for the topology changes of the interface induced by the relative motion between the gas and liquid phase. Therefore, the complex fluid dynamic process during drop ejection is simulated with CFD package FLOW-3D that employs the VOF method to track effectively the transient fluid interface deformations and disruptions. VOF method utilizes a finite difference to represent the free surfaces and interfaces that are arbitrarily oriented with respect to the computational grids. The VOF defines a volume fractional function F that indicates the fraction of the computational cell filled with liquid, and uses a donor-acceptor algorithm to track the interface. There exists a free surface interface while the value of F is between zero and unity in a cell. Although VOF can locate the free boundary nearly as well as a distribution of marker particle method and needs less information-stored space, the method is worthless unless an algorithm can be devised for accurately computing the evolution of the F field. The time dependence of F is governed by

$$\frac{\partial F}{\partial t} + F\nabla \bullet \vec{V} = 0 \tag{1}$$

The mass and momentum equations can be written as the conservation form and homogeneous as follows

$$\frac{\partial \rho}{\partial t} + \nabla \bullet (\rho \vec{V}) = S_c \quad , \tag{2}$$

and

$$\frac{\partial \vec{V}}{\partial t} + (\rho \vec{V} \bullet \nabla)\vec{V} = -\nabla P + \nabla \bullet \tau_{ij} + S_m \quad , \tag{3}$$

where ρ is the density, t is the time, P is the pressure, $\vec{V}$ is the velocity vector, F is the volume fraction function, τ_{ij} is the viscous stress tensor, and S_c, S_m are the source terms.

In the numerical simulation model, FLOW-3D© is used as the simulation tool. The thermal bubble dynamics model used in FLOW-3D is an advanced homogeneous bubble model and programming in the CFD codes. The model describes that the bubbles obey the homogeneous bubble rule, i.e. the pressure and temperature of the bubble are spatially uniform. The equation of state for the thermal bubble is the ideal gas and is expressed as follows.

$$p_v = (\gamma - 1)\rho C_V^{vap} T_v \tag{4}$$

where p_v is the bubble pressure, C_V^{vap} is the specific heat at constant volume of the vapor, γ is the ratio of specific heats for the gas, and T_v is the bubble temperature.

When no heat flux crosses the interface between the heater and ink, phase change begin to occur on the interface of bubble and liquid. It is necessary to have a relation that expresses the saturation pressure of the vapor, P^{sat} in terms of temperature. The common relationship is the Clapeyron-Clausius equation

$$P^{sat} = P_{V1} \bullet \exp[-(\frac{1}{T} - \frac{1}{T_{V1}}) / T_{V\exp}] \tag{5}$$

where P_{V1} is saturation pressure of the vapor, T_{V1} is saturation temperature of the vapor, and $T_{V\exp}$ is an exponent constant given by

$$T_{V\exp} = (\gamma - 1)C_V^{vap} / C_{LHV1} \tag{6}$$

where C_{LHV1} is the latent heat of the working fluid.

Results and Discussion

In order to investigate and compare the difference of ejection performance between top- and back-shooting designs of the firing chamber, five type of firing chamber is designed in this study for two of fluid feed inlet channels. Figure 1 shows the five types of models for firing chambers and micro-fluid channel geometries. Type-A and B models are the back shooting designs while the Type-C, D and E models with the top shooting designs. For the back shooting design, there are two heaters within the firing chamber for Type-A model and an additional heater on the neck of the inlet channel for Type-B model. The two heaters are located on the side wall of the firing chamber and each of the heater area size is 13 μm × 6.5 μm. The heater area size located on the neck of the inlet channel is 11 μm × 11 μm. While for the top shooing design, there are two heaters for Type-C model, which are the same heater sizes with Type-A model. Type-D model is the top shooting design with only one heater with the heater size of 13 μm × 13 μm, which is the same with the over all of two heaters design within the firing chamber for comparison. Model of Type-E is the same with Type-D model but with an additional heater on the neck of the inlet channel.

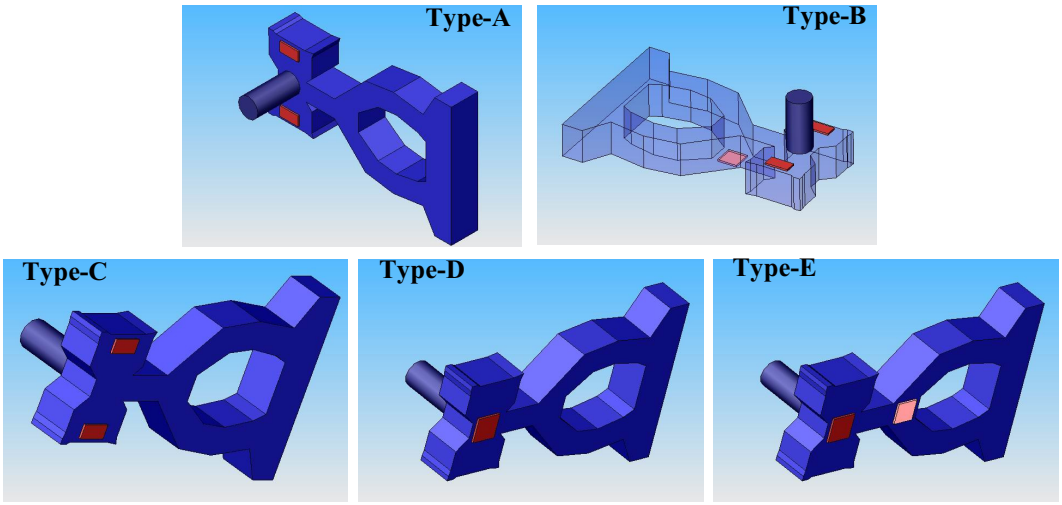

Figure 1. Models of firing chamber for Type-A and B of back shooting design and Type-C, D and E of top shooting design

In this study, the working fluid is water and its physical properties are 1.01 g/cm^3, 1.0 cps and 72.8 dyne/cm for density, viscosity, and surface tension, respectively. The initial nucleation pressure inside the thermal bubble is 10 MPa (about 100 atm), which is the typical initial condition of thermal bubble inkjet. Figure 2 shows the computational results of Type-A model for firing chamber at the instant of 0, 5 and 10 µs and the results in two-dimensional X-Y sectional plane is shown in Fig. 3. Figure 4 also shows the results of Type-A firing chamber in Y-Z cross sectional plane at 0, 2, 4, 6, 8 and 10 µs. The average droplet ejection velocity of the computational result is 12.24 m/s. Figure 5 shows the computational results of Type-B model for firing chamber at 0, 5, and 10 µs and the results of Type-B model for firing chamber in Y-Z sectional plane at 0, 5, and 10 µs is shown in Fig. 6. The average droplet ejection velocity of the computational result is 13.5 m/s and with a longer droplet tail than the result of Type-A model. However, the growing and collapsing force of thermal bubble on the neck heater of Type-B model cause the tail of the droplet not in the straight direction when leaving the nozzle surface. It may increase the probability of droplet puddling on the nozzle plate surface even for increasing the ejection speed of droplet. Figure 7 shows the results of Type-A and Type-B model for firing chambers in two-dimensional Y-Z cross sectional plane at 7 µs. The velocity increase for Type-B model is about 11% than the Type-A model, which is caused by the additional of heater locate on the neck of the inlet channel.

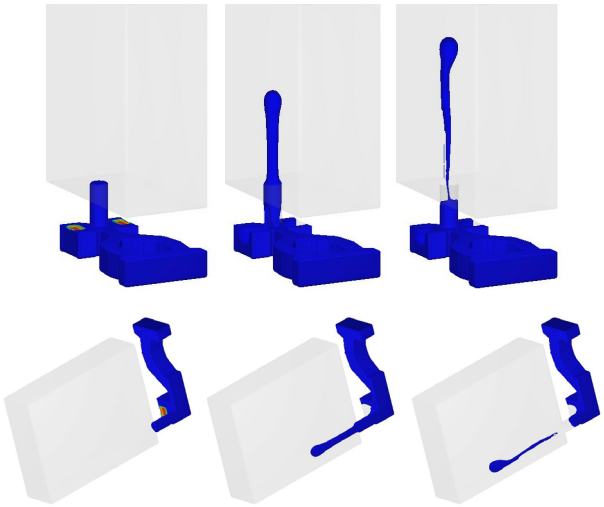

Figure 2. Computational results of Type-A firing chamber at 0, 5, and 10 µs

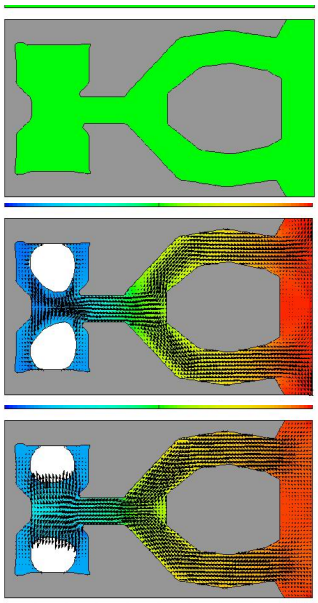

Figure 3. Computational results of Type-A firing chamber in X-Y 2D section plane at 0, 5, and 10 µs

Figure 8 shows the results of Type-C model for firing chamber at 0, 5, and 10 µs. Type-C model is the top shooting design with two heaters inside the firing chamber and the droplet ejection velocity is 12.14 m/s. Figure 9 shows the computational results of Type-A and Type-C model in two-dimensional Y-Z sectional plane at the instant of 7 µs. The ejection velocities for both the Type-A and C are almost the same for both the back- and top-shooting designs, respectively, with two heaters inside the firing chamber. The results of Type-D model for firing chamber at the instant of 0, 5, and 10 µs, which is shown in Fig. 10. It reveals that the average droplet ejection velocity of the computational result is 14.9 m/s. Figure 11 shows the computational results of Type-C and Type-D firing chambers in two-dimensional Y-Z sectional plane at 7 µs. The velocity increase for Type-D model is about 42% than the Type-C model, which is caused by the one heater design just below the nozzle hole and located on the geometry center of the firing chamber. Figure 12 shows the computational results of Type-E model for firing chamber at 0, 5, and 10 µs. It reveals that the average droplet ejection velocity of the computational result is 17.4 m/s, which is the largest ejection speed among the five types of firing chamber designs.

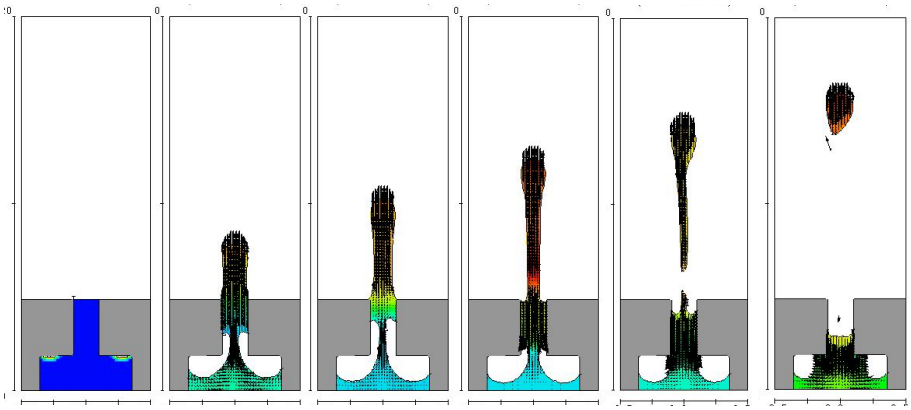

Figure 4. Computational results of Type-A firing chamber in Y-Z 2D section plane at 0, 2, 4, 6, 8 and 10 µs

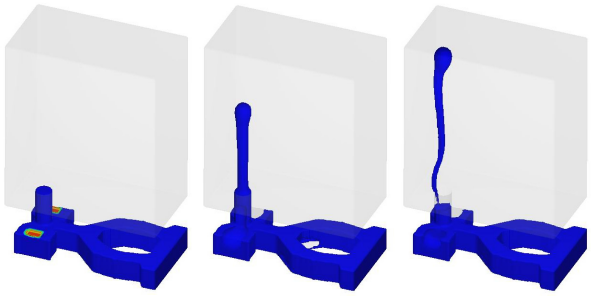

Figure 5. Computational results of Type-B firing chamber at 0, 5, and 10 μs

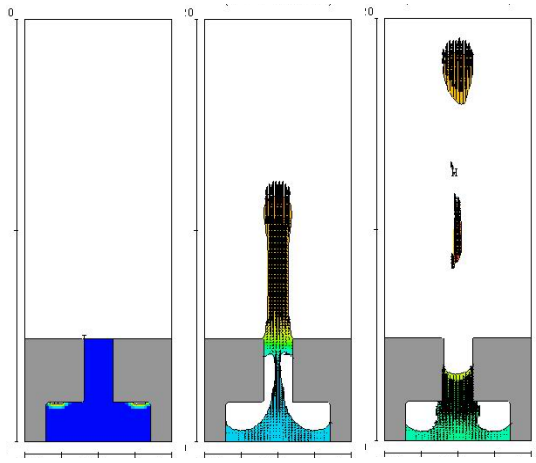

Figure 6. Computational results of Type-B firing chamber in Y-Z 2D section plane at 0, 5, and 10 μs

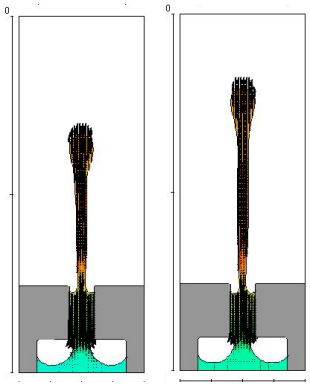

Figure 7. Computational results of Type-A and Type-B firing chambers in Y-Z 2D section plane at 7 μs

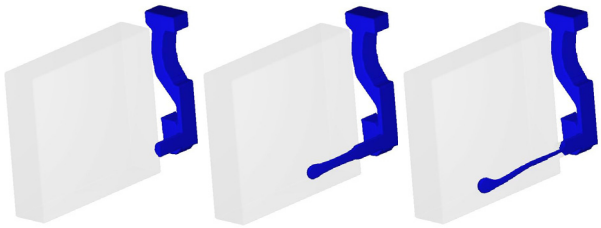

Figure 8. Computational results of Type-C firing chamber at 0, 5, and 10 μs

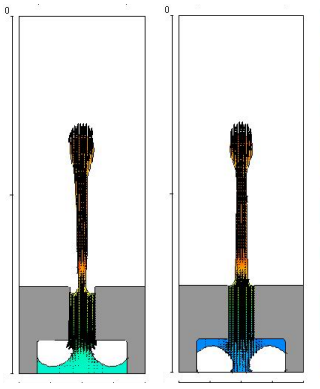

Figure 9. Computational results of Type-A and Type-C firing chambers in Y-Z 2D section plane at 7 μs

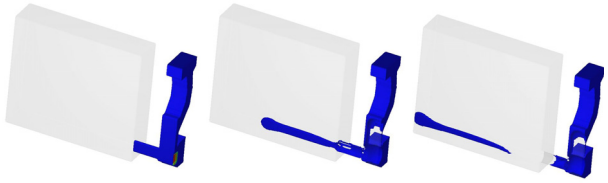

Figure 10. Computational results of Type-D firing chamber at 0, 5, and 10 μs

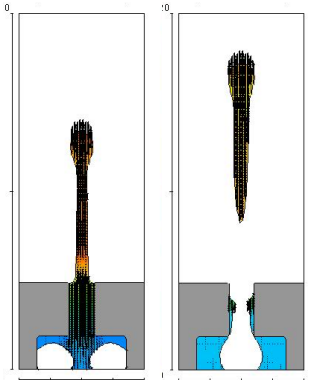

Figure 11. Computational results of Type-C and Type-D firing chambers in Y-Z 2D section plane at 7 μs

Figure 12. Computational results of Type-E firing chamber at 0, 5, and 10 μs

Conclusion

Back-shooting type design of inkjet print head could have a non-assembly packaging process and it may solve the miss alignment problem between the inkjet chip and nozzle plate, especially for higher density array of thermal bubble heaters. Therefore, ejection performances for both the top-and back-shooting type designs are investigated and compared in this study by using the CFD method. In order to study the difference of ejection performance between top- and back-shooting designs, five types of firing chamber is designed in this study for two of fluid feed inlet channels. The average droplet ejection velocity of the computational result is 13.5 m/s of Type-B model and with a longer droplet tail than the result of Type-A model. However, the growing and collapsing force of thermal bubble on the neck heater of Type-B model cause the tail of the droplet not in the straight direction when leaving the nozzle surface. It may increase the probability of droplet puddling on the nozzle plate surface even for increasing the ejection speed of droplet. Velocity increase for Type-D model is 42% than Type-C model, which is caused by the one heater design just below the nozzle hole and located on the geometry center of the firing chamber. The average droplet ejection velocity of Type-E model design is the largest ejection speed among five types of the firing chamber designs.

References

1. Asai, A., Hara, T., and Endo, I., 1987, One-dimensional Model of Bubble Growth and Liquid Flow in Bubble Jet Printers, Jpn. J. Appl. Phys., Vol. 26, pp. 1794-1801.
2. Chen, P. H., Chen, W. C., Chang, S. H., 1997, Bubble growth and ink ejection process of a thermal ink jet print head, Int. J. Mech. Sci., Vol. 39, pp. 683-695.
3. Yang J.C., Chiu C.L., and Chang C.C., "Operating Voltage Effects on Bubble Growth Dynamics of Thermal Inkjet Print heads," IS&T's NIP18: 2002 International Conference on Digital Printing Technologies, pp.153-156, San Diego, California, USA (2002).
4. Chiu C.L,. Yang J.C, Liu C.H., Hu J.P., and Chang C.C., 2001, "The Numerical Study on Size Effects of the Inkjet Print Heads," IS&T's NIP17: International Conference on Digital Printing Technologies, pp.319-322, Fort Lauderdale, Florida, USA (2001).

Biographies

Jinn-Cherng Yang jointed the Printing Technology Division of OES/ITRI in 2001. He received his M.S. and Ph.D. from Institute of Aeronautical and Astronautical Engineering of National Cheng Kung University. His interest lies in the turbulent flow field of computational fluid dynamics, numerical simulation of two-phase flow. He is the section manager of Print Head Testing Section.

Chi-Ming Huang joined the printing Technology Division of OES/ITRI in 2002. He received his M.S. degree from Institute of Applied Mechanics of National Taiwan University, Taipei, Taiwan. His current research includes MEMS technology, thin film process and the study of monolithic inkjet head.

Chun-Jung Chen joined the Printing Technology Division of OES/ITRI in 1990. He received his M.S. degree from Department of Power Mechanical Engineering of National Tsing Hua University, Hsinchu, Taiwan. His interest lies in electro-photography, media handling of printer and magnetic damper. He is the department manager of Printing Device Department in OES/ITRI.